MDI Measurement Errors: The Magnetic Perspective
SOI-Technical Note 01-144

Y. Liu & A.A. Norton

W.W. Hansen Experimental Physics Laboratory, Center for Space Science and Astrophysics, Stanford University, Stanford, CA 94305-4085

yliu@quake.stanford.edu

norton@quake.stanford.edu

1. Introduction

This Tech Note addresses MDI error analysis and data difficulties from the magnetic perspective. Nevertheless, results are applicable to helioseismology studies.

2. Line Profiles and Model Dependency

Line profiles can be computed by resolving Unno-Beckers equations through solar atmosphere. MDI uses the spectral line Ni-I 6767.772 $\mathring{A}$ that is formed by the transition from the z^3P^o state at 3.6576 eV excitation energy to the meta-stable a^1S state at 1.8262 eV, showing doublet Zeeman splitting by 30.5 m$\mathring{A}$/kGauss with g=1.426 (Bruls et al. 1993). A solar atmosphere model, the Harvard-Smithsonian Reference Atmosphere (HSRA) (Giggerich, et al. 1971), is used here to calculate line profiles. The Stokes parameters *I, V* and *Q* based on HSRA model are shown in the upper two rows in Figure 1. The color lines represent different strengths of magnetic field that are from 0 Gauss to 4000 Gauss. The inclination angle and azimuthal angle of the magnetic field are 30 degree and 22.5 degree respectively. The location of the region is 30 degrees away from solar center. Linear polarized lights along the horizontal and vertical directions are shown in the third row and the RCP and LCP in the bottom row. The dashed lines are the positions where MDI samples the intensities F1-4.

MDI measures horizontal linear polarized light, as well as circular polarized lights, to get Dopplergrams. While intensities at four positions are sampled, an algorithm is employed to obtain an index that relates to velocity. Such an index is calibrated to velocity using a look-up-table. The Dopplergram from circular polarized lights is the average of LCP and RCP measurements and the magnetogram is the differences of those two.

Simulation shows that using circular polarization to measure velocity (see Figure 2) is much better than using linear polarization (see Figure 3), but the dynamic range of circular polarization is a little bit smaller than the linear one when magnetic strength turns out to be large (see Figure 4). The reason is when magnetic field becomes stronger, the line profile of the linear polarization turns out broader and shallower that is much different from the standard profile used for calibration while the line of circular polarization shifts left or right that is sometimes out of sampling positions. When the magnetic field is not extremely high, such as lower than 2000 Gauss, the error of velocity measurement is less than 15% using linear polarization and less than 5% using circular polarization.

The error of magnetic field measurement is less than 10% generally (see Figure 5), but would dramatically increase when velocity exceeds a certain value. For example, the error of 4000 Gauss measurement will be 600 Gauss when the speed reaches 2000 m/s.

The simulation is model dependent. When a sunspot model (Maltby et al. 1986) is used (see Figure 6), the measurement using horizontal linear polarization becomes much better (see Figure 7).

Simulation shows that two factors, magnetic field and velocity, are convolved each other in calibration. Considering solar rotation up to 2000 m/s and speed of satellite up to 600 m/s, the maximum background velocity is 2600 m/s. The velocity and magnetic field measurements with circular and linear polarizations have satisfied accuracy if the magnetic field is not stronger than 2000 Gauss. When magnetic field is extremely strong, say higher than 3000 Gauss, circular polarization measurement can give reasonable values in low velocity zone while linear polarization measurement is questionable.

In summary, MDI provides reliable velocity and magnetic field measurements when magnetic field is lower than 2000 Gauss. The velocity and magnetic field are underestimated up to 5% and 15% respectively by means of using circular and linear polarizations. Observation of velocity and magnetic field in umbra would be reasonable using circular polarization though 20% - 30% underestimated when the sunspot is near solar center. The velocity observation will induce up to 100% error using linear polarization if magnetic field is higher than 3000 Gauss. The scattered light and focus problem will cause other uncertainty so the error would be higher, especially in umbra. We will discuss those issues later.

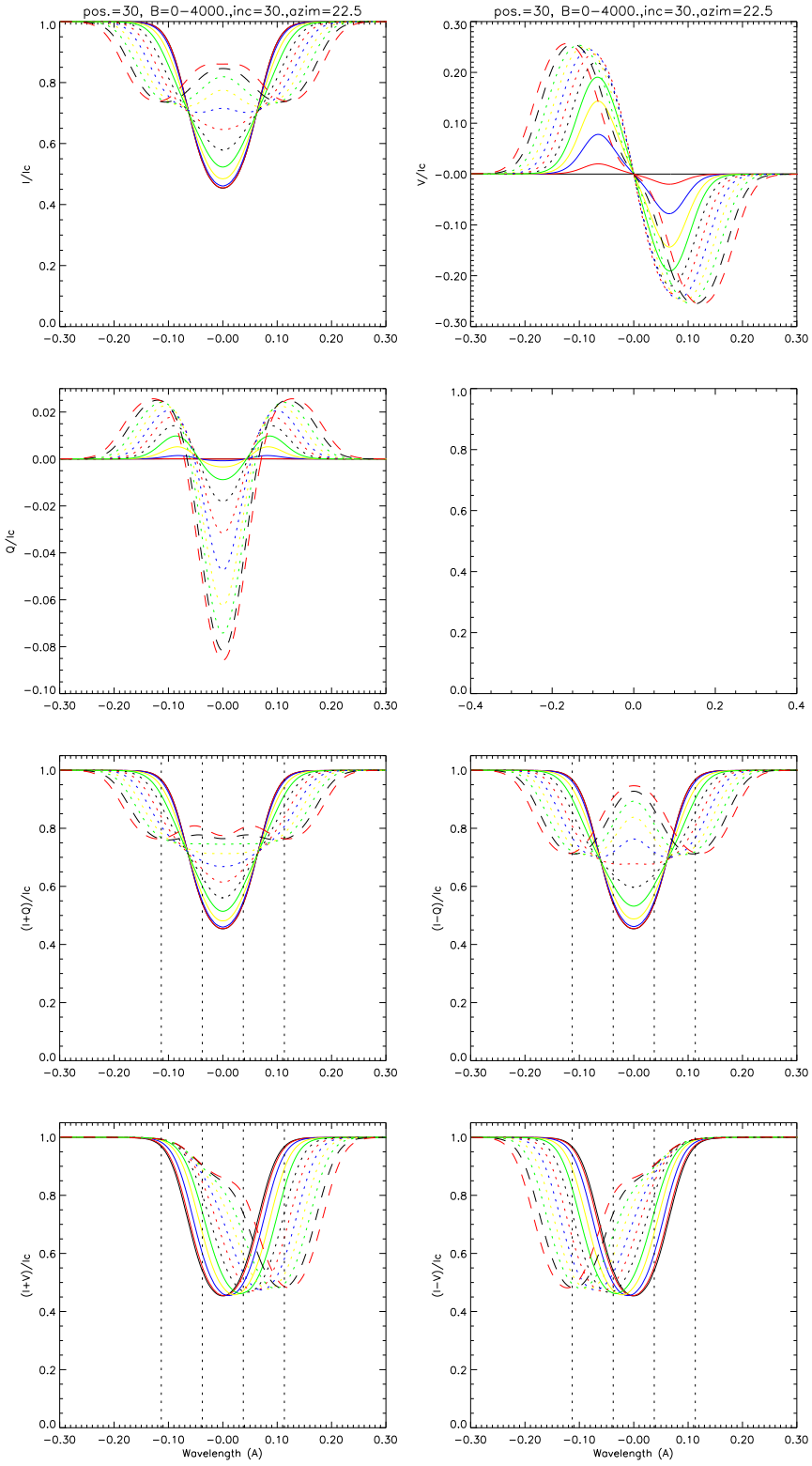

Fig. 1.— The Stokes parameters calculated from HSRA.

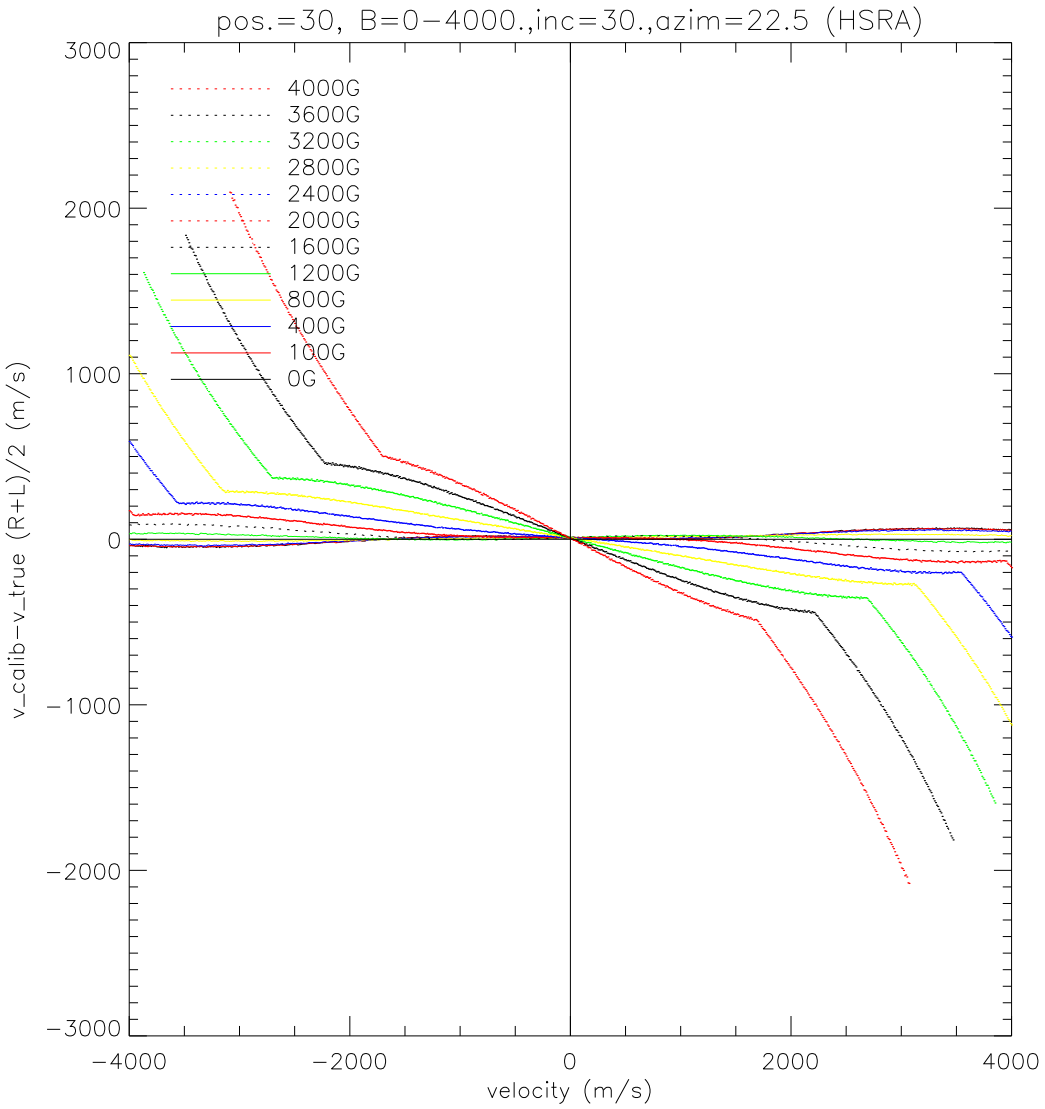

Fig. 2.— Velocity error versus velocity using circular polarization and HSRA model.

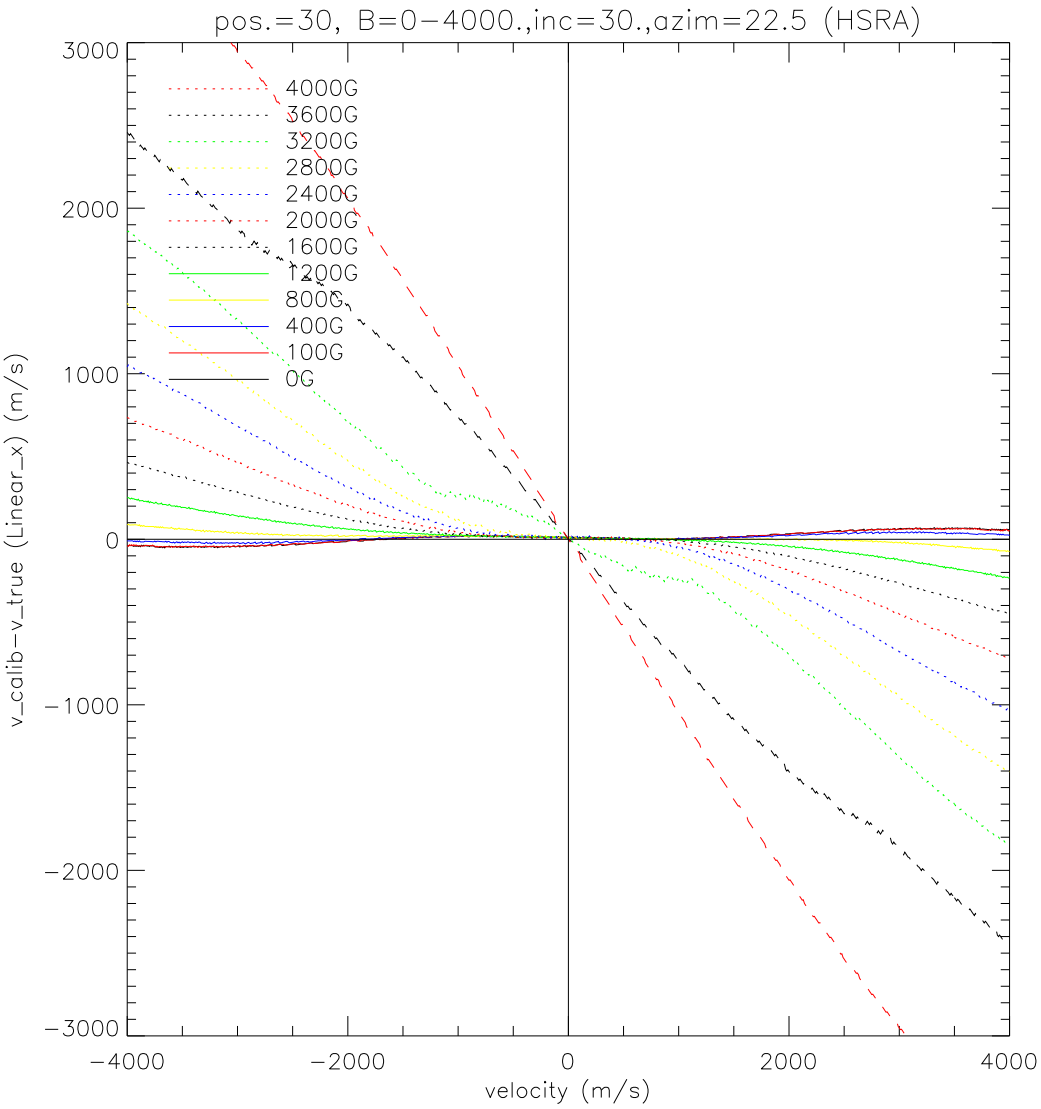

Fig. 3.— Velocity error versus velocity using horizontal linear polarization and HSRA model.

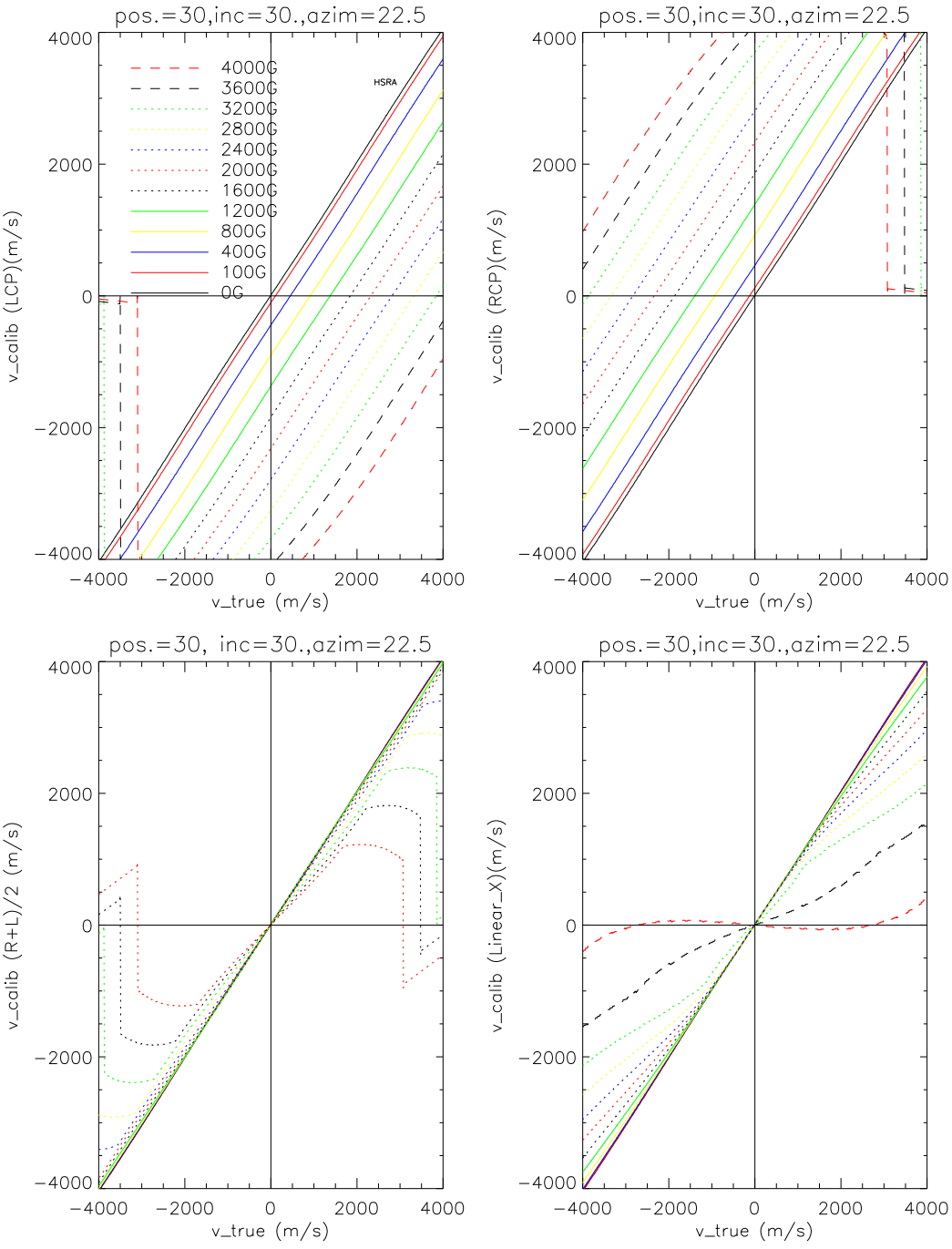

Fig. 4.— The top row panels show velocity measured by RCP and LCP versus real velocity. The bottom two are the average of velocity of RCP and LCP versus real velocity and the velocity measured by horizontal linear polarization versus real velocity. The measurement using circular polarization is much better than using linear one, but the dynamic range is smaller when magnetic strength becomes strong.

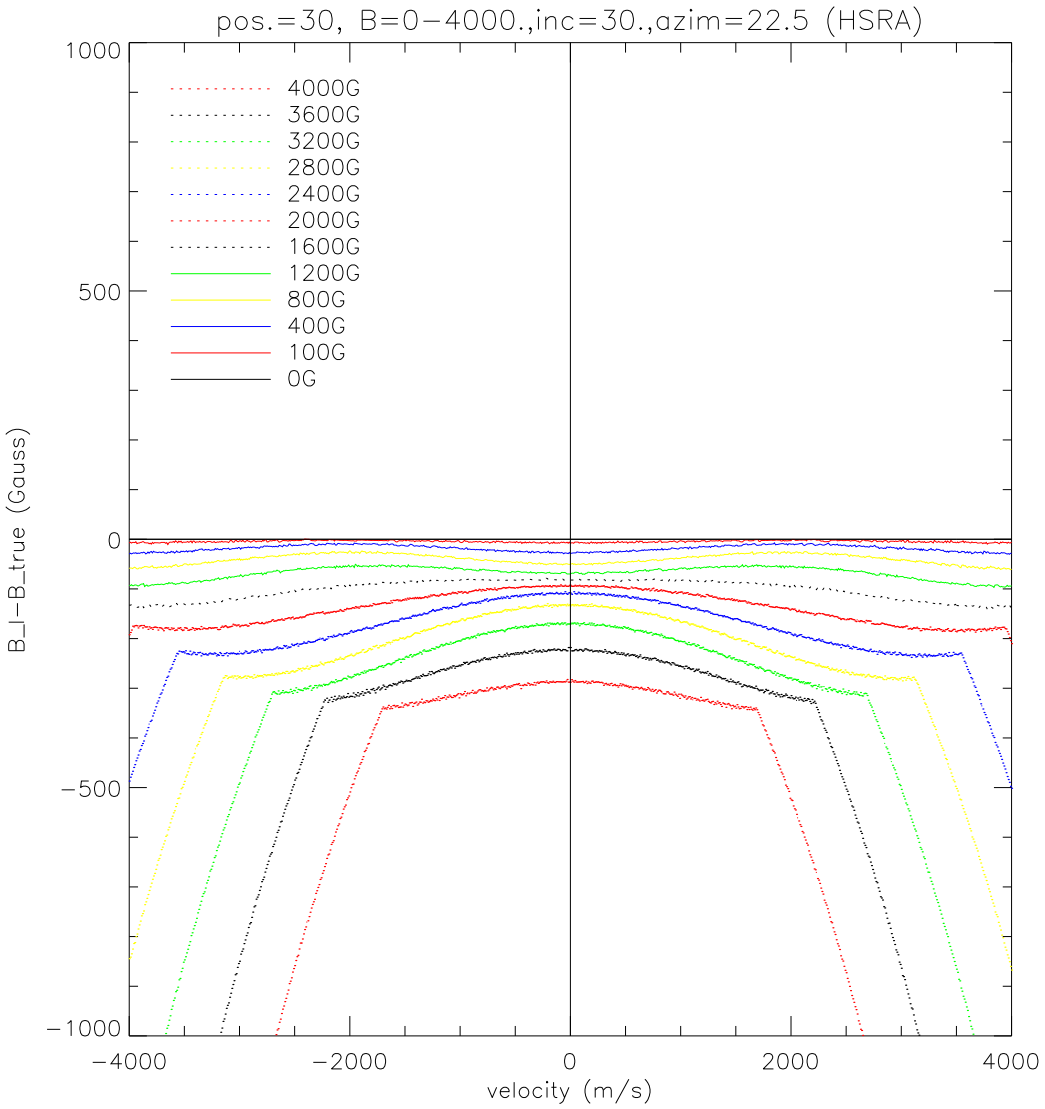

Fig. 5.— Magnetic field error versus velocity using HSRA model.

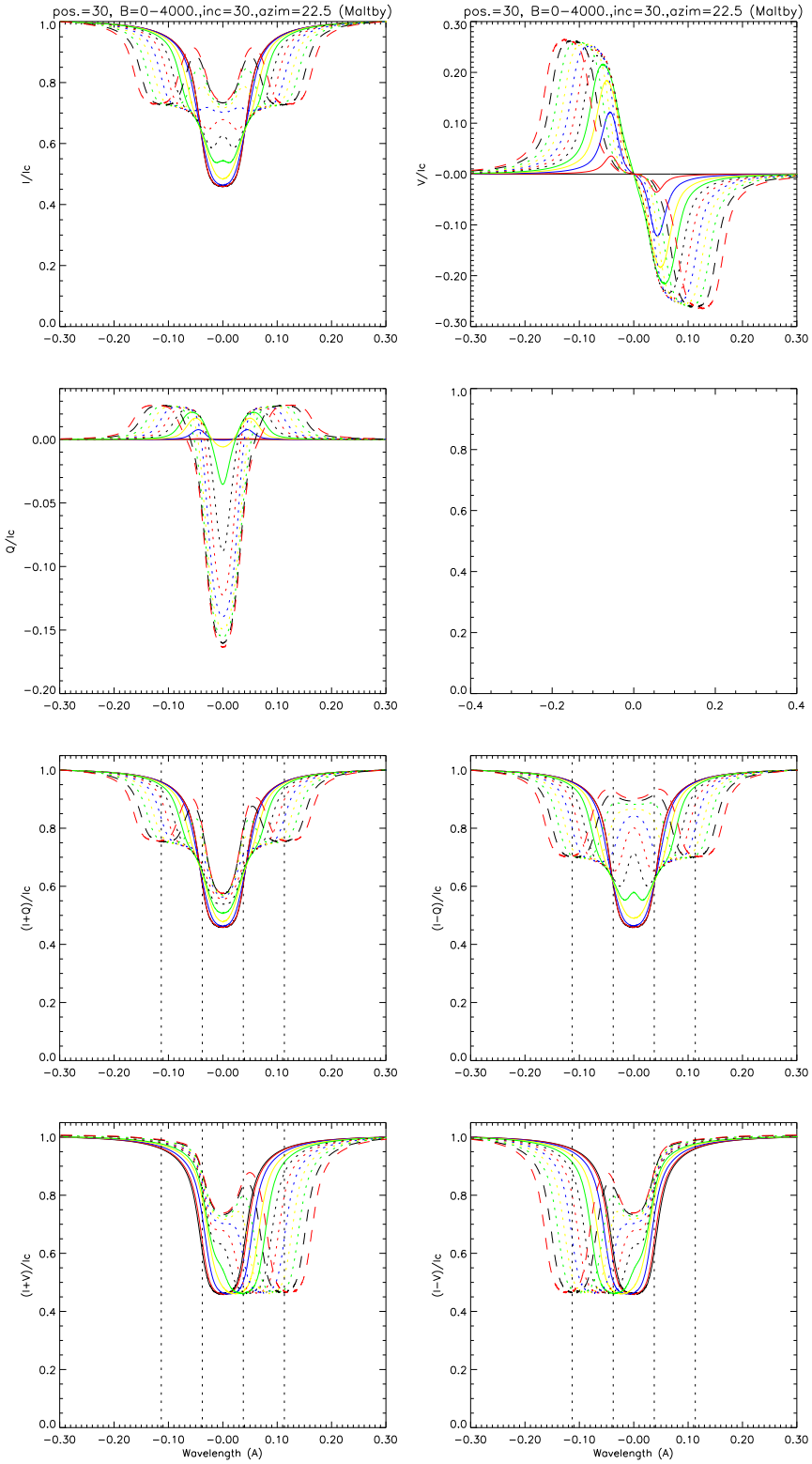

Fig. 6.— As same as in figure 1 using Maltby sunspot model.

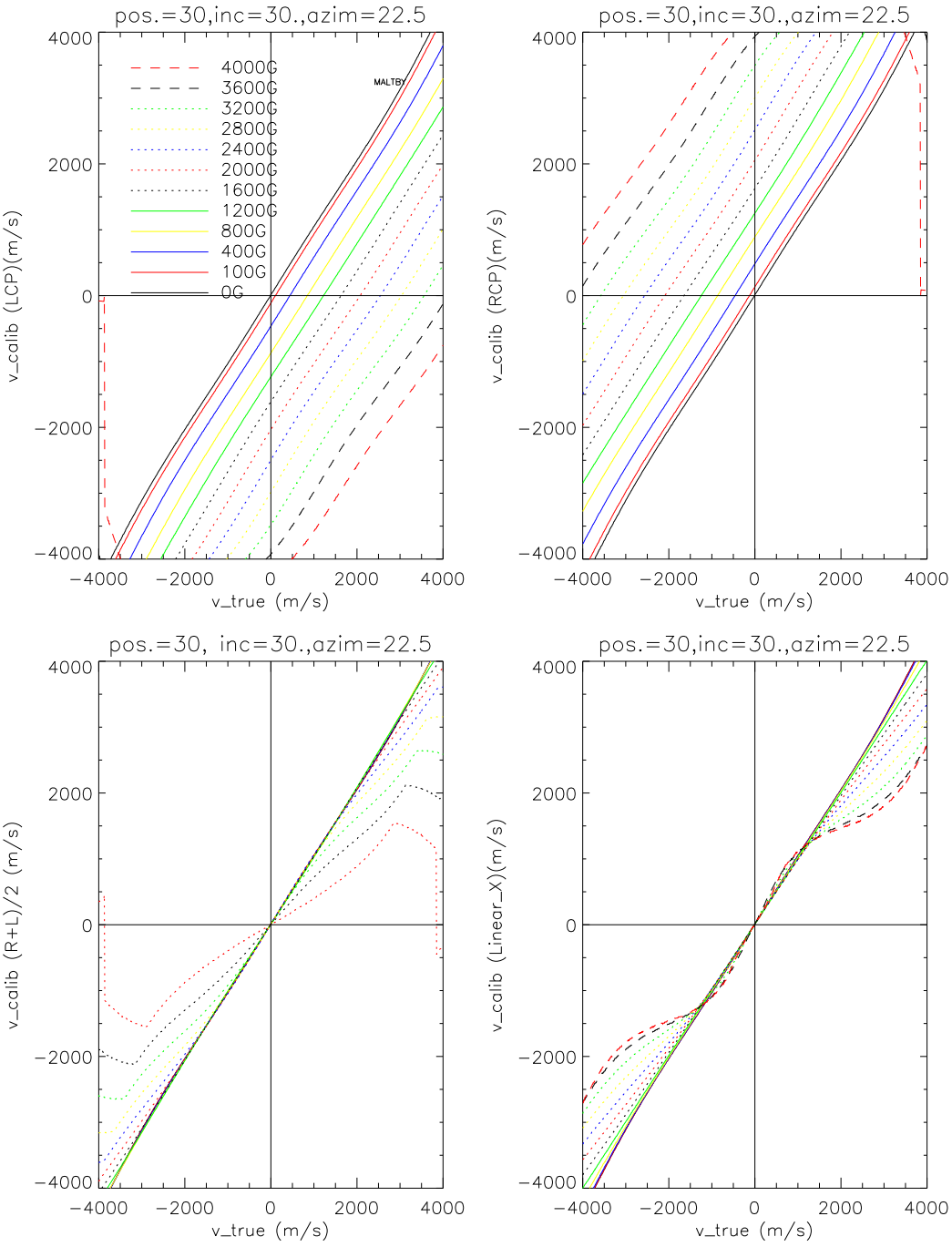

Fig. 7.— As same as in figure 4 using Maltby sunspot model.

3. Low Light Levels

MDI data has proven problematic in some sunspot umbra, where magnetic flux drastically decreases to values of several hundred Gauss, instead of the kGauss level expected (see Figure 8). The effect was inaccurately referred to as "saturation" for years and was understood by many to be a result of the RCP and LCP line profiles moving beyond the wavelength sampling range of the filtergrams due to large magnetic field strengths and/or large velocities. The working range of wavelength sampling for no magnetic field and for umbral strength field is seen in Figure 9 and 10. This explanation proved incorrect as it became apparent that the MDI algorithm broke down for umbral strength fields only when the combined spacecraft and rotational velocity were greater than 2000 ms^{-1}, as shown in Figure 10. This rationale could not be applied to MDI data because saturation was observed in sunspot umbra at disk center when rotational velocity was minimal and also when the spacecraft velocity was near zero. An example of saturation in sunspot umbra at disk center can be found in the upper right and lower left panels of Figure 8.

The real cause of problematic umbral values began to be understood with a closer examination of the data. All datapoints which showed contaminated values had extremely low intensity values, see Figures 11 and 12. It is known that a relationship exists between field strength and continuum intensity. Darker regions having stronger fields (Lites et al. 1991; Martinez & Vazquez 1992). Scattered light was investigated as the cause of the contamination, but could not account for the severity of the problem.

Finally, this problem was understood when data from a "line profile" campaign was found which contained a sunspot exhibiting "saturation". The line profile data was gathered through the campaign "cam_hr_vel_lp_e256" conducted on 20 May 2000. The data from the line profile campaign was compared to an MDI magnetogram taken roughly the same time: hr_M_1024x500_01h.64714. Strikingly, the line profiles did not look like they were contaminated with scattered light. Instead, a calculation which mimicked the calculation on board MDI but was not exactly the calculation, returned reasonable values for the magnetic field and velocity within the problematic umbral pixels. But when the values were run through the MDI on-board processing algorithm, a large error appeared for certain data which had very low intensity values, see Figure 13 to compare the line profile data to the MDI on-board processed data.

It was discovered that a floating point calculation done on board the MDI spacecraft contained a limiting algorithm. In order to investigate the problem, the "vcalc" program (which does the MDI velocity method to 4 filtergrams input) was modified to do the on-board calculation in 16-bit shorts as well as in doubles. The parameter "passes" sets the number of passes over the line in the summed input filtergrams. Passes can be 1, 2, or 4

to mimic on-board calculations. If passes=0 then the calculation is done in doubles. The same on-board velocity lookup table is used in both cases. The lookup table is found at: /home/soi/tables/MDI_Vlookup.fits.

Using the modified vcalc program, it was verified that the on-board calculation made the "saturation" problem more severe than what was seen in the line profile data. But it is also clear that the values within the umbra are problematic regardless of the floating point error.

The reason for the problem is not so much a bug as a limitation of the algorithm. The calculation is done as specified in Tech Note 110 and works over the range of parameters given there. The problem is that the intensity and line depth drop significantly in the umbra (see Figure 14). Remember the method uses the ratio Ssum/Sa or −Sc as an index into the MDI_Vlookup table. Ssum is (F1+F2) − (F3+F4) i.e. the blue side minus the red side intensity. Sa is F1-F3 and Sc is F2-F4. For the expected line parameters, Sa or Sc are zero at ±1800 m/s. At that velocity the other of Sa or Sc will be large (or rather should be large if there is a line present). The choice of which denominator to use is based on the sign of Ssum. If Ssum is >0, then Sa is used. Note that Ssum will be >0 when the line is to the red of the Michelson tuning center. When this is the case, Sa should be large. The range expected is 100 to 1000 (where the continuum is 3000).

In the particular umbra examined, Sa drops to 50. When Sa drops below 96 the reciprocal table saturates at 32767 (it is a 15 bit table returning a 2s complement short, the table is made by dividing 3×2^{24} by the index). This saturation of the reciprocal is the source of the difference between on-board and on-ground calculations. In the sample spot both LCP and RCP velocities are in error in the umbra. Ssum drops to about 75 and Sa drops to 50. Even if the normalizing Sa^{-1} were not limited to 32767 because Ssum is so small the velocity will be wrong because the lookup table is built assuming a line depth similar to that found in quiet sun. All four filtergrams converge to the same small value in the umbra of this spot - i.e. the line is almost gone (see Figure 14).

So, there are two problems (see Figure 15):

1. When the intensity gets very small and/or the line gets weak the reciprocal table lookup saturates so the "alpha" will be too small. A factor of 2 in this example. About 750m/s error due to this saturation.

2. When the line depth decreases as fraction of continuum the velocity table is wrong and the velocity will be too small by an unknown (at the moment) but probably significant amount - again some hundreds of m/s.

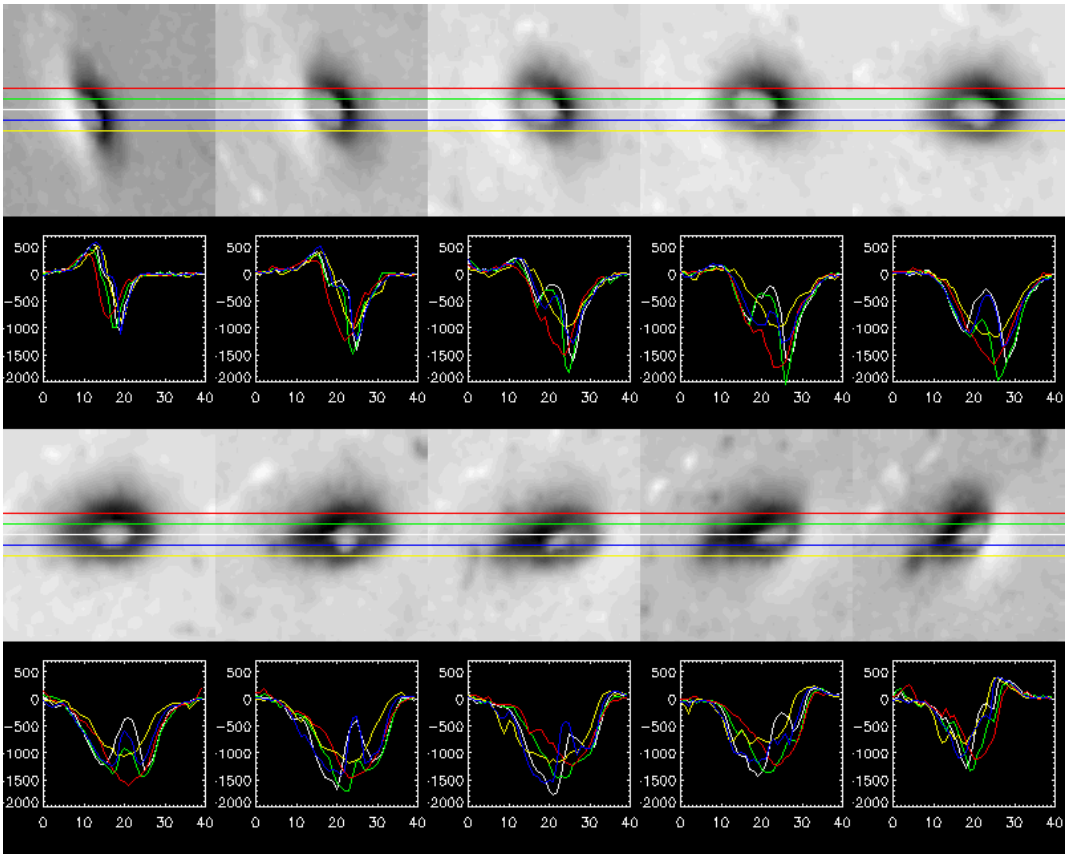

Fig. 8.— Grayscale images of a northern hemisphere sunspot in late December of 1999. "Saturation" is seen at each center-to-limb position as the sunspot crosses the disk. X-slices of data are shown below each image to show variations in magnetic field values and the severity of contamination.

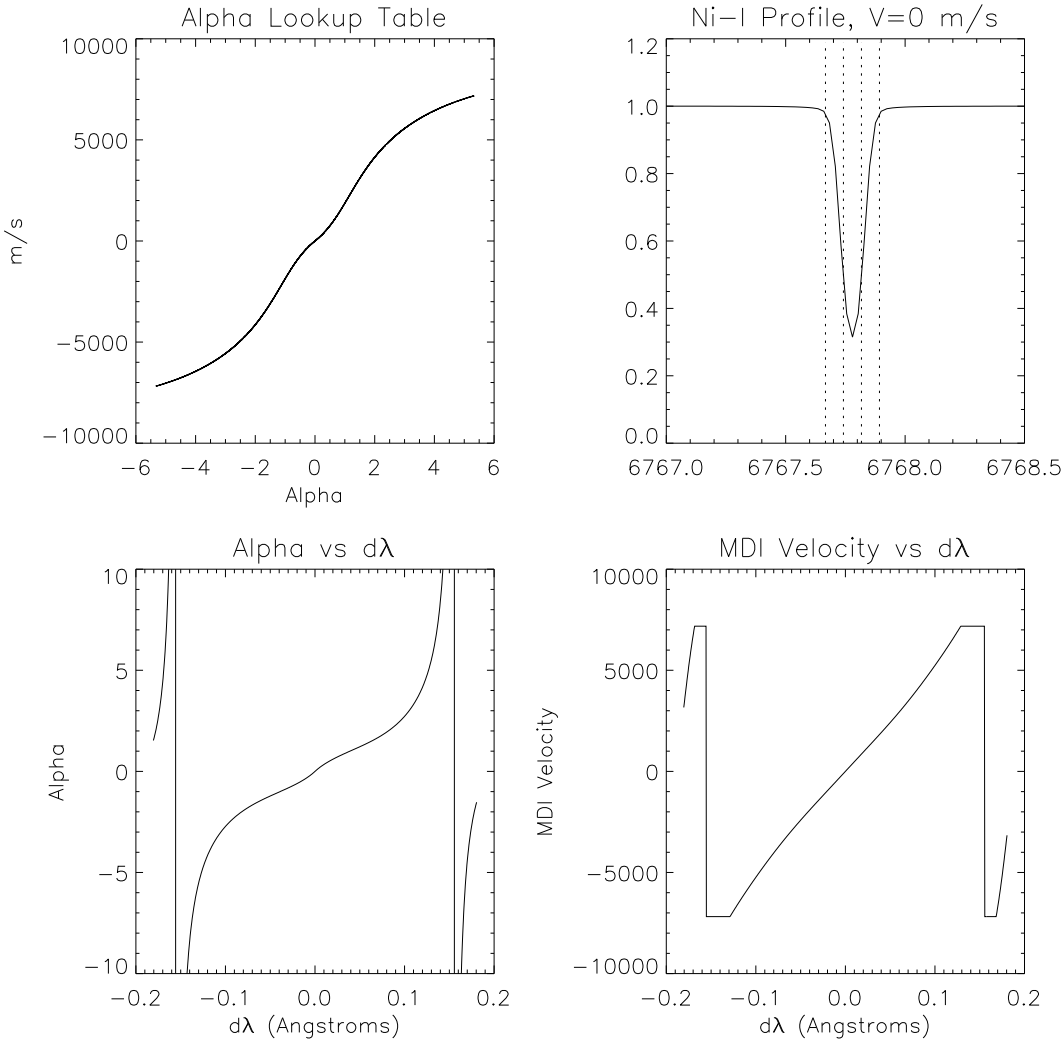

Fig. 9.— The alpha lookup table (upper left) and the Ni-I line profile (upper right) corresponding to a zero velocity and zero magnetic field are shown. A shift in central wavelength position (dλ) of the line returns a specific alpha value (lower left). The useful alpha range for such a profile is shown (lower right), $\approx \pm$ 0.14 Å.

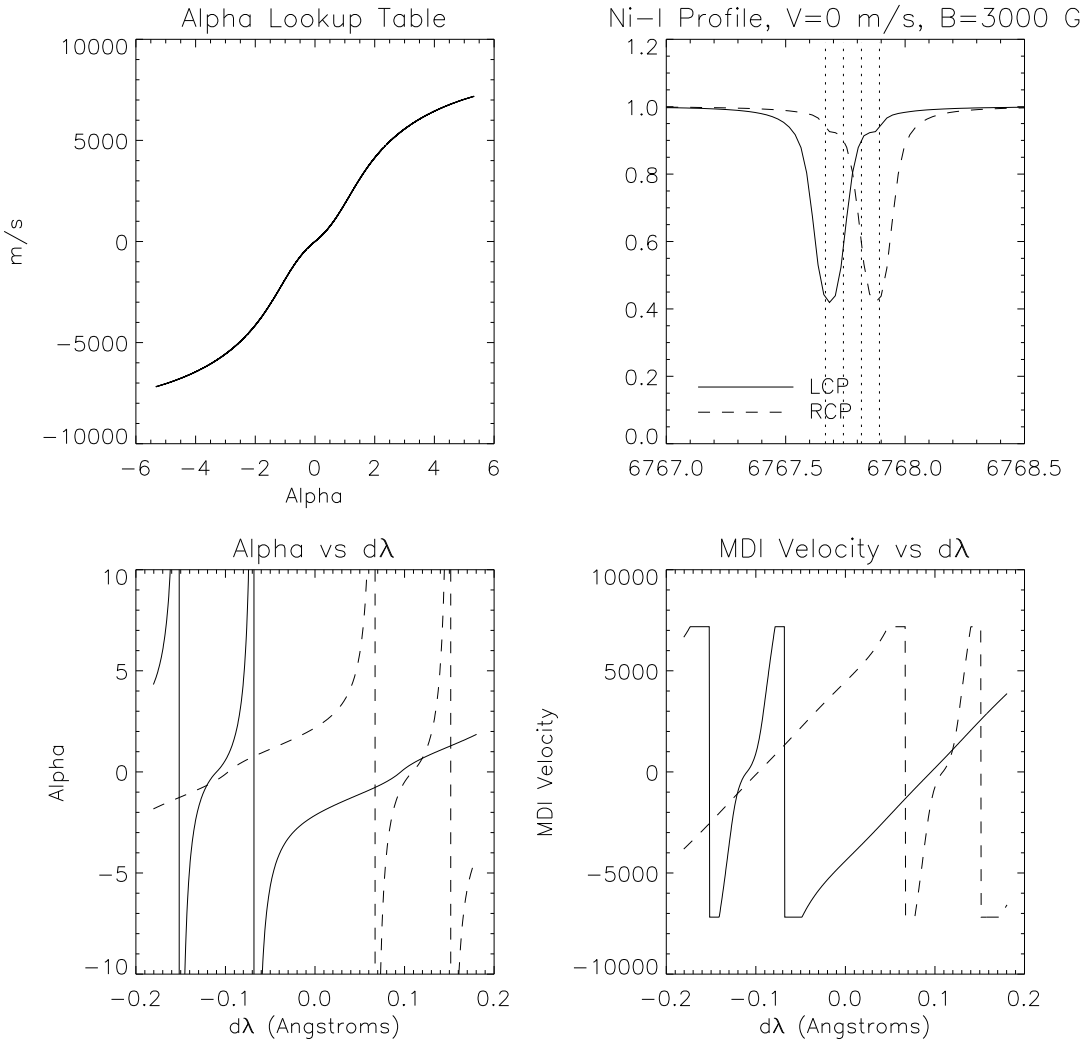

Fig. 10.— The alpha lookup table (upper left) and the Ni-I LCP and RCP line profiles (upper right) corresponding to a zero velocity and 3000 Gauss magnetic field are shown. A shift in central wavelength position (dλ) of the line returns a specific alpha value (lower left). The useful alpha range for such a profile is shown (lower right), reduced from previous example to $\approx\pm$ 0.06 Å.

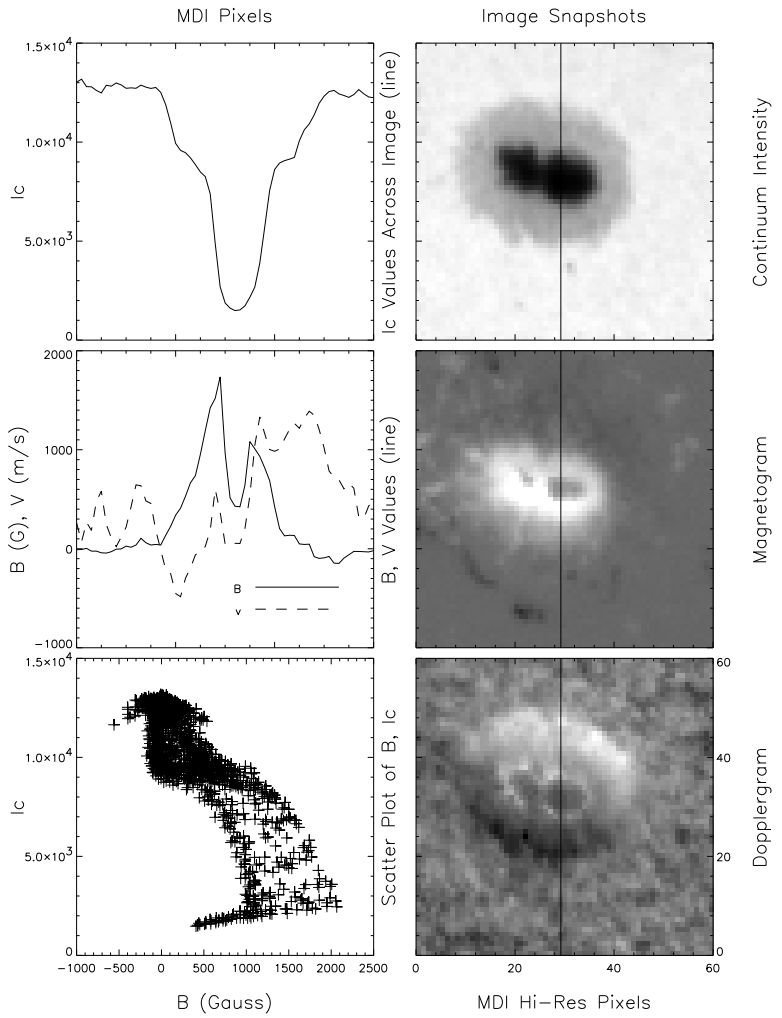

Fig. 11.— Representative MDI data: y-slices (upper left) and snapshots (right) for full-disk data from Dec 24, 1999 clearly show umbral contamination. Velocity (lower right) is derived from linearly polarized light and quite clearly shows contamination. Most importantly, the sharp demarkation of erroneous data in intensity versus field strength scatter plot (lower left) shows the contamination stems from low light levels.

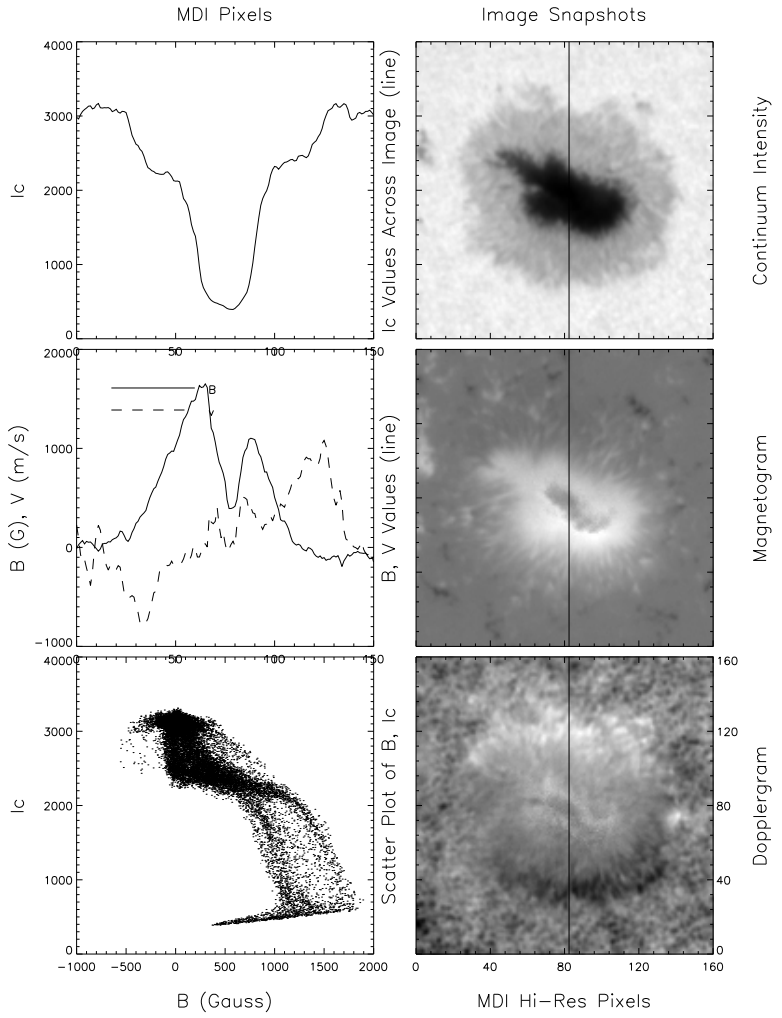

Fig. 12.— Representative MDI data: y-slices (upper left) and snapshots (right) for hi-res data from Dec 24, 1999 clearly show umbral contamination. Velocity (lower right) is derived from circularly polarized light. Most importantly, the sharp demarkation of erroneous data in intensity versus field strength scatter plot (lower left) shows the contamination stems from low light levels.

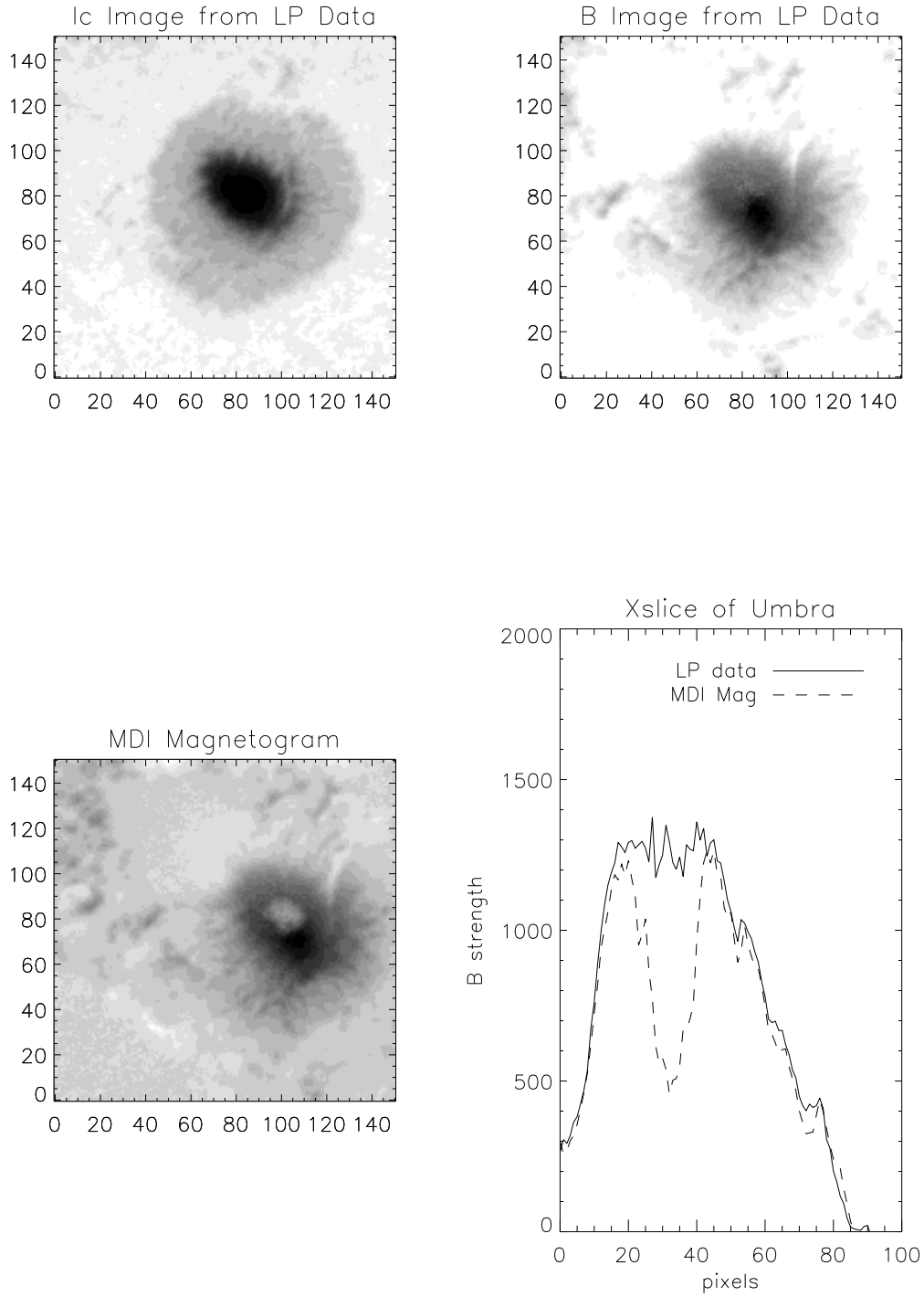

Fig. 13.— Comparison of line profile data (top panels) to the MDI magnetogram (lower left). The differences in values are plotted in lower right panel.

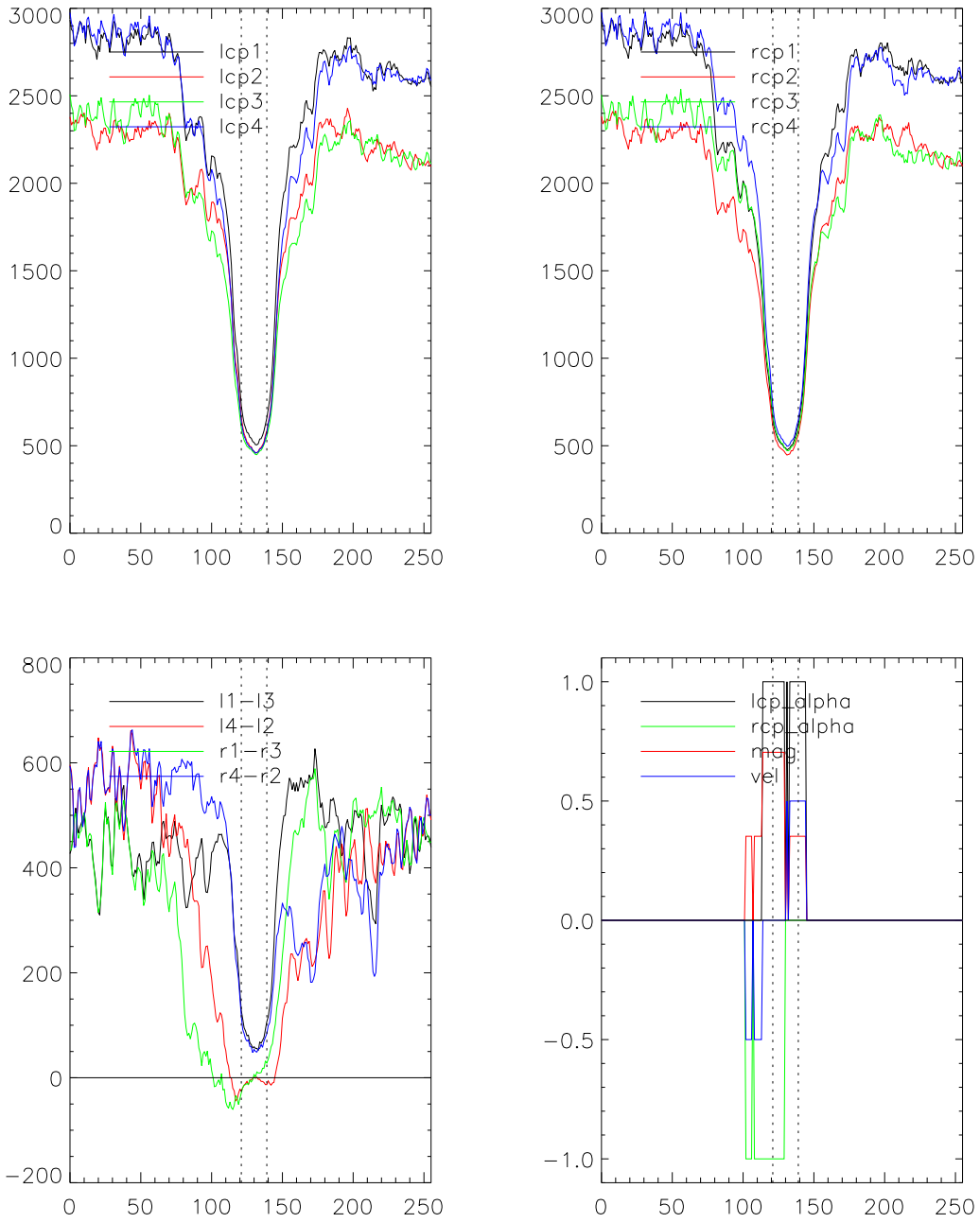

Fig. 14.— MDI measures intensities in the line profile campaign. The region between the dashed lines is where the 'saturation' appears.

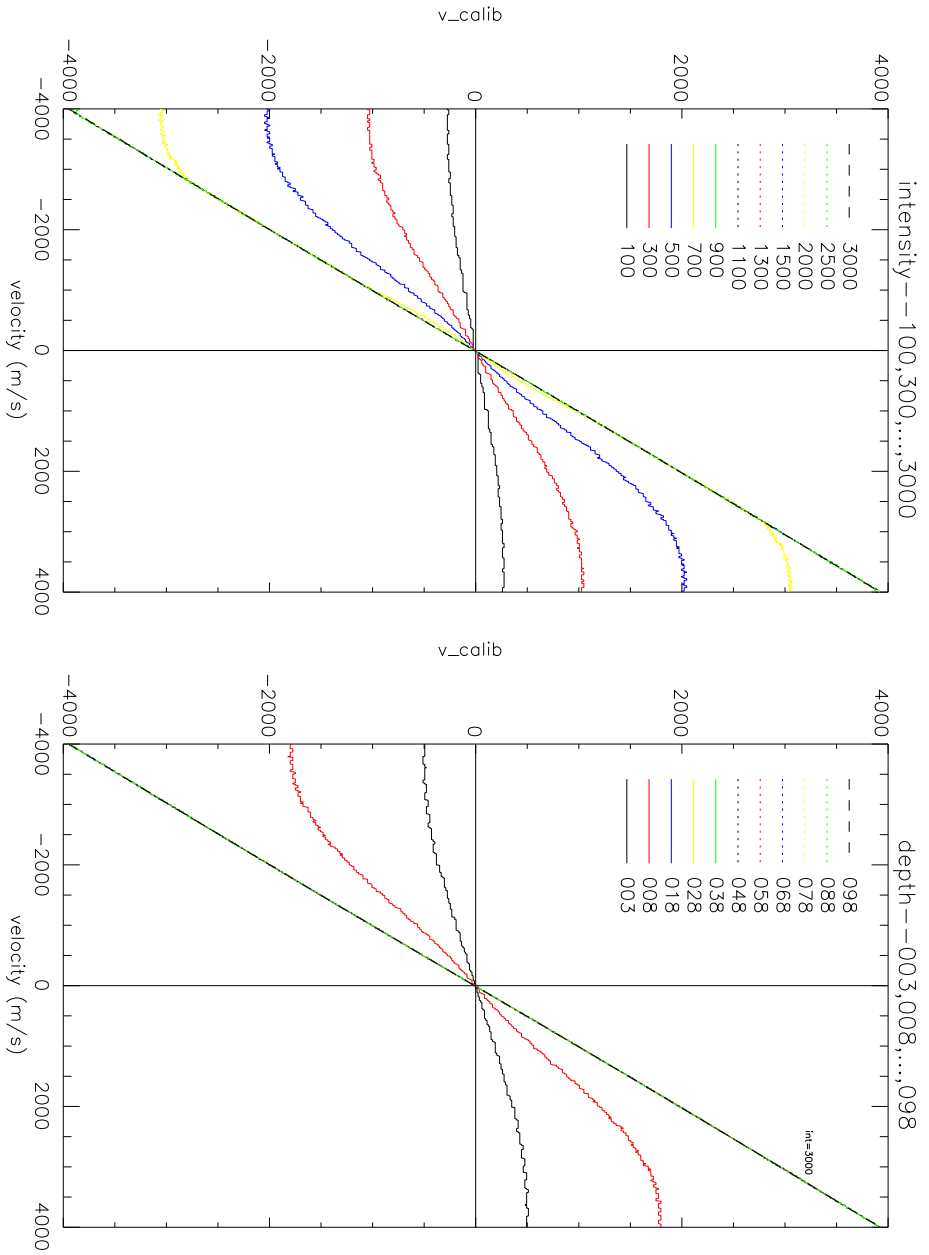

Fig. 15.— The dependency of intensity and velocity measurement. left panel: The calibrated velocity depends on the intensity; right panel: the calibrated velocity versus different line depths.

4. Scattered Light

Investigation into scattered light in MDI images was motivated by a need to understand comtamination of umbral data. A quick look at spatially uncropped intensity images from I0 filtergrams (which is a measure of the continuum intensity) provided an estimate for scattered light by looking at how quickly the intensity dropped off beyond the solar limb. A limb-darkening function (Pierce & Slaughter 1977) was compared with data. The intercept point, where the limb function values intercepted the data as shown in upper left panel of Figure 16, was used to determine the solar limb position. This rough estimate of scattered light yielded a function as seen in upper right panel of Figure 16.

I find values of 0.019 (% of disk center intensity) $10''$ off the limb with values of 0.664 (% disc center intensity) $1'$ interior to limb. Roughly, the values are doubled, since umbra has scattering from "both sides": so $2\times0.019/0.664$ gives 0.057, or roughly 6%. But I'm not sure this estimate is applicable in umbra as penumbral scattering will be coming from 10-$20''$ away instead of $1'$. A better estimate might be the limb intensity value or, $2\times0.019/0.368$ which is closer to 10%. Therefore, 10% of penumbral intensity ($\approx$10000 counts) is scattered into an area with intensity values less than 1400 counts. Given possibly a 5% scattered light contribution from the quiet sun, that leaves very little light originating from the umbra itself. These estimates warranted a further look at the data to determine how the percent contributions affect the line profiles and MDI algorithm results.

A comparison of scattered light measured off the limb to the point spread function (PSF) of the instrument as derived by Rabello-Soares et al. (2001) is shown in the lower panels of Figure 16. Rabello-Soares et al. (2001) (data labelled as MCR in Figure 16) used continuous intensity images sampled 4 per day: observable named fd_Ic_6h_01d. This particular PSF was calculated for June 1st, 1996. The main different is the shape of the line, an Airy function for MCR results and a Gaussian for off-limb measurement (AAN).

MDI intensity and longitudinal magnetic field data exhibiting contaminated umbral values from 12.24.99 (northern hemisphere sunspot) are studied. First, the contaminated data is removed from the images and replaced by more reasonable estimates. The magnetic field values within the umbra are fit with a Gaussian so that strongest field values are central. According to the estimates of scattered light (explained above), 90% of the light is removed from the contamined pixels in intensity images.

The top panels of Figure 17 show data with contamination removed. X-slices through the data are shown in middle panels: real MDI data with contamination is shown as dotted line, doctored MDI data with contamination removed is shown as solid line, results from applying the measured PSF to the data are shown as overlaid points. Applying the measured

PSF to the data was done as follows: The 2-dimensional (20×20 pixels) PSF was applied to each position of an MDI intensity image. The total intensity value was determined by summation of all counts. The magnetic contribution from all pixels to the total value for any given pixel was determined by percentage of total counts contributed multiplied by field strength. (This assumes that the magnetic flux determined by the MDI algorithm can be derived from a line profile which is a summation of the contribution of its parts based on total percentage of intensity. This assumption has not been tested.) This method yields results which appear similar to contaminated data (see Figure 17 lower panels). The PSF was then altered slightly to see if an exact replica of contaminated data could be acheived. The best matches to contaminated data were found when the far tail of the PSF was lowered and the width of the Gaussian narrowed a bit, as seen in the lower panels of (see Figure 16) which actually plot the 'best results' PSF and compares it with one measured by Rabello-Soares et al. (2001).

Further studies of the line profiles (see §3) showed that scattered light was not the primary problem in umbral contamination.

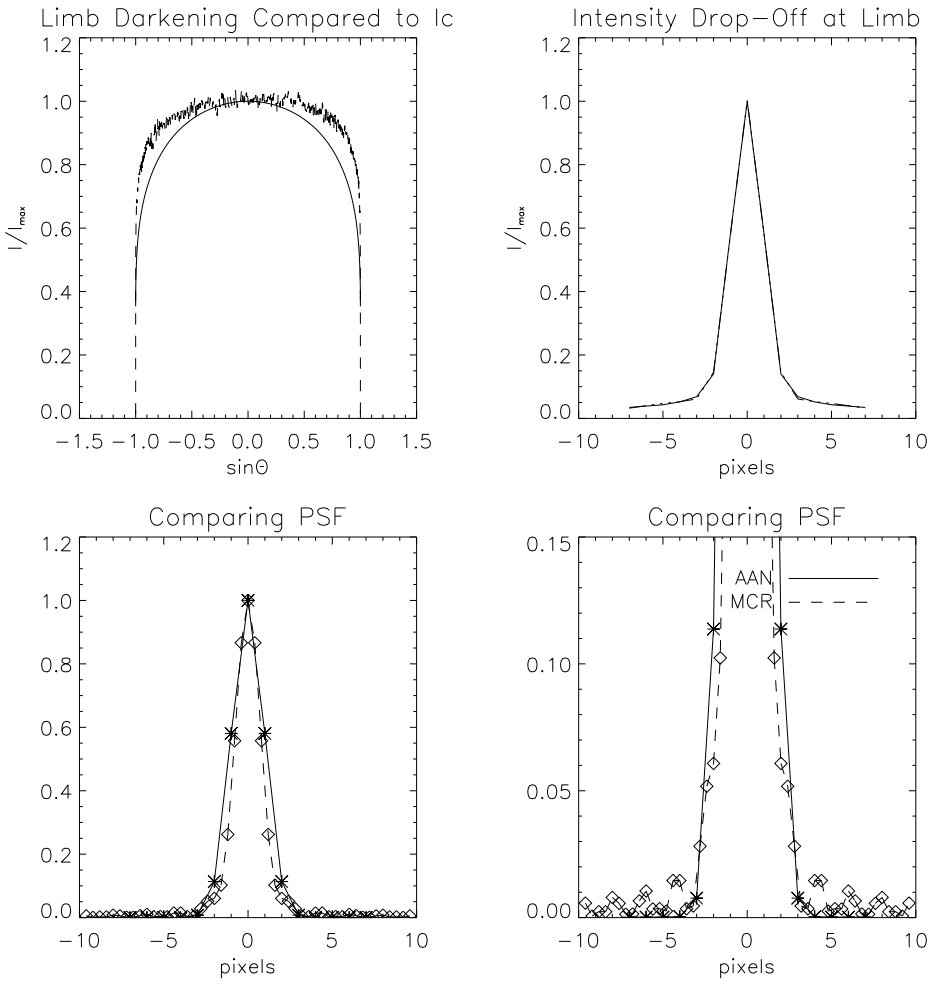

Fig. 16.— A comparison of the limb-darkening function and the observed limb function (upper panels). The profile measured off the limb is then plotted as compared with a point-spread function determined for MDI (lower panels).

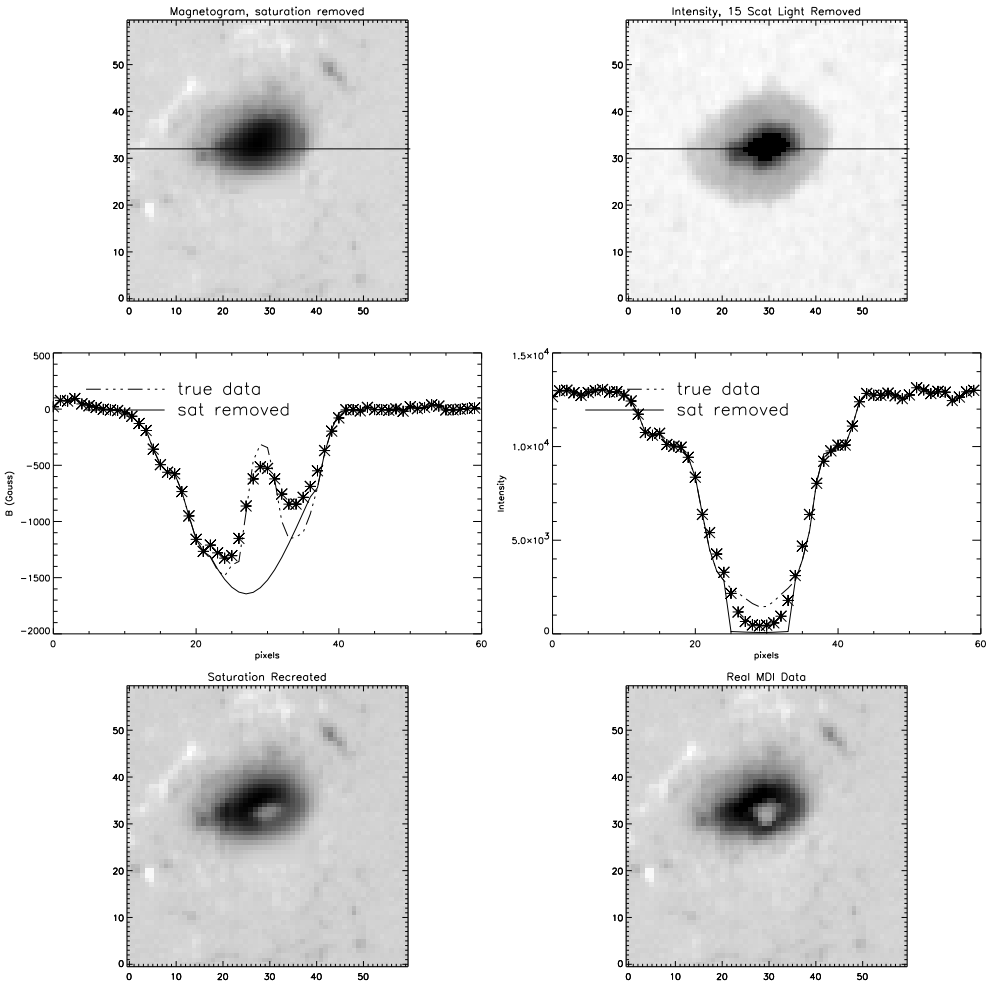

Fig. 17.— Using a modified point spread function for the MDI instrument and convolving it with umbral data (which has contamination removed: upper panels) can produce an effect (lower left) similar to that seen in "saturated" MDI data (lower right). X-slices through the data are shown (middle panels).

5. Filtergram Cadence

Imaging a large spatial field has the disadvantage of not sampling the spectral line simultaneously. Therefore, physical processes present in the solar atmosphere can develop and change during the finite amount of time it takes to complete an observation. MDI observables are the result of a combination of filtergrams taken over a 30 second period. Systematic errors in magnetic field measurements with a Fabry-Perot interferometer reported by Settele et al. (2001) motivated an examination of errors introduced by the MDI filtergram cadence.

Assuming predominant line profile changes during observing time are caused by p-modes, I test the effect an underlying sinusoidal velocity signal has on MDI velocity and magnetic measurments. I begin with an artifical Stokes I and V profile from Ni-I calculated by SIR (Stokes Inversion Code) with the Maltby-M umbral model atmosphere given a 2000 Gauss field. I also generate an artificial sinusoidal velcoity with a period of 300 seconds and a given amplitude. The MDI measurement is simulated through use of the michelson and lyot filter functions used in conjunction with the line profile shifted every 3 seconds (which is the rate the MDI filtergrams are taken) in order to simulate an underlying velocity. This test ignores the fact that solar oscillations are a combination of modes.

The sequence of filtergrams during a magnetogram campaign are: I1Lcp, I1Rcp, I2Rcp, I2Lcp, I0, I3Lcp, I3Rcp, I4Rcp, I4Lcp, I0. Where I1-4 describe the filtergram measurement position along the line profile, Lcp denotes left circularly polarized light and Rcp denotes right circularly polarized light. I0 are the continuum filtergrams taken in standard polarization. The filtergrams are taken every 3 seconds so that an observation sequence is 30 seconds in duration. The resultant filtergram values are combined in the usual manner (Scherrer et al. 1995). An alpha is determined for the left circularly polarized data: sa=L1−L3, sc=L2−L4, ssum=sa+sc and alpha=ssum/−sc or if ssum>0 then alpha=ssum/sa. The same is done using right circularly polarized data to determine an alpha. Using the alpha lookup table, two velocities are determined, one for the right and one for the left circularly polarized profiles. The magnetogram value is: B=(Right Velocity−Left velocity)/2.84. The velocity in circularly polarized light is (Right Velocity+Left velocity)/2.0.

Note that during a magnetogram campaign, the velocity which is downlinked may be an average of the right and left circularly polarized profile velocities, but more often, the velocity observable is a result of the previous 30 second observation termed 'structure'. Structure observations use standard polarization with a cadence as follows: I0, I1, I2, I3, I4, I4, I3, I2, I1, I0. Therefore, to simulate any relationship between velocity and magnetic fields, one needs to consider that the values are derived from different observing sequences 30 seconds apart. I include velocity values from linearly polarized light in order to be thorough.

It appears that the MDI filtergram cadence in combination with an underlying velocity imparts an oscillatory component to the magnetic field strength, see Figure 18. The solid line represents the artificial sinusoidal velocity with a 300 second period and the dashed red line is the variation of the magnetic field strength introduced by the distortion of the line profile during the measurement time. The magnetic field strength plotted in Figure 18 has the average field value subtracted, magnetic amplitude shown on the left axis. The introduced magnetic oscillation is -90 degrees out of phase with the velocity oscillations. The RMS amplitude of the input velocity was selected to be on the order of what is observed by MDI in sunspot umbra (Norton, A.A. 2000). Observed MDI signals are plotted in lower panel of Figure 18 for comparison purposes from a 1355 G field strength pixel.

Figure 19 plots the observed MDI v and B signals along with the expected B signal from the cadence effect. The observed velocity (solid line in Figure 19) is interpolated onto a 3 second time grid and used to shift the line profile an appropriate amount at each filtergram measurement. The produced B oscillation (red dotted line) from shifting a 1355 G line profile according to the velocity and sampling the filtergrams at the MDI cadence does not mimic the B signal as measured by MDI. I hand selected a signal from an MDI pixel whose (v, dB) phase was exactly that expected from the cadence effect, therefore this example represents the worst case scenario, or the data most likely contaminated. In reality, (v, dB) phases in MDI data have a wide range of values (Norton, et al. 2001). The expected B amplitude is often less than half of the observed amplitude, as well as being out of phase. It does not appear that the MDI B oscillation is heavily contaminated by this effect.

Further simulations show the expected amplitudes introduced into MDI magnetic measurements as a function of input velocity amplitude and field strengths, see Figure 20. Field strengths used to compute line profiles are 600, 800, 1000, 1800, 2000 and 2200 Gauss. The introduced magnetic error increases with increasing velocity amplitude and increasing field strength values. Also plotted in Figure 20 are symbols representing average RMS values of velocity and magnetic field strength as observed with MDI on November 10, 1999 when a bipolar active region was in the hi-res field of view. The signals were detrended with a gaussian, width of 30 minutes. Then the signals were filtered so for the 5 minute bandwidth. The RMS amplitudes were binned according to their Gauss values (0-50 G, 50-100, 100-150,....1700-1750 G). Each point on the graph corresponds to average RMS v and B values for increasing field strength. It is obvious that observed MDI B oscillations are greater than expected errors introduced by the cadence effect.

Conclusions from this study are as follows.

- MDI filtergram cadence in combination with an underlying velocity imparts an oscillatory component to the magnetic field strength, see Figure 18.
- Oscillatory component to field strength always has a phase value of (v, dB)=−90 degrees. The maximum introduced RMS amplitude is a function of velocity amplitude and field strength, but realistic errors are on the order of 5/2000 G, or 0.25%.
- The cadence of observation also offsets the velocity values (roughly 20%) in circularly polarized light, seen as blue line in Figure 18.
- The cadence effect increases the observed amplitude for velocity values derived from linearly polarized light, seen as points in Figure 18.
- It does not appear that the magnetic signal measured by MDI is a smaller-amplitude echo of the velocity signal shifted by −90 degrees, see Figure 19. Although there is a relationship between velocity and magnetic oscillations, as would be expected if motions in the photosphere are jostling the flux tubes, the observed B signals do not show the predictable phase expected from this velocity-cadence effect. The magnetic signal often appears to be independent of the velocity and have large amplitudes when the velocity does not and vice versa.
- RMS amplitudes of field strength observed by MDI are much greater than that predicted by this effect, see Figure 20.

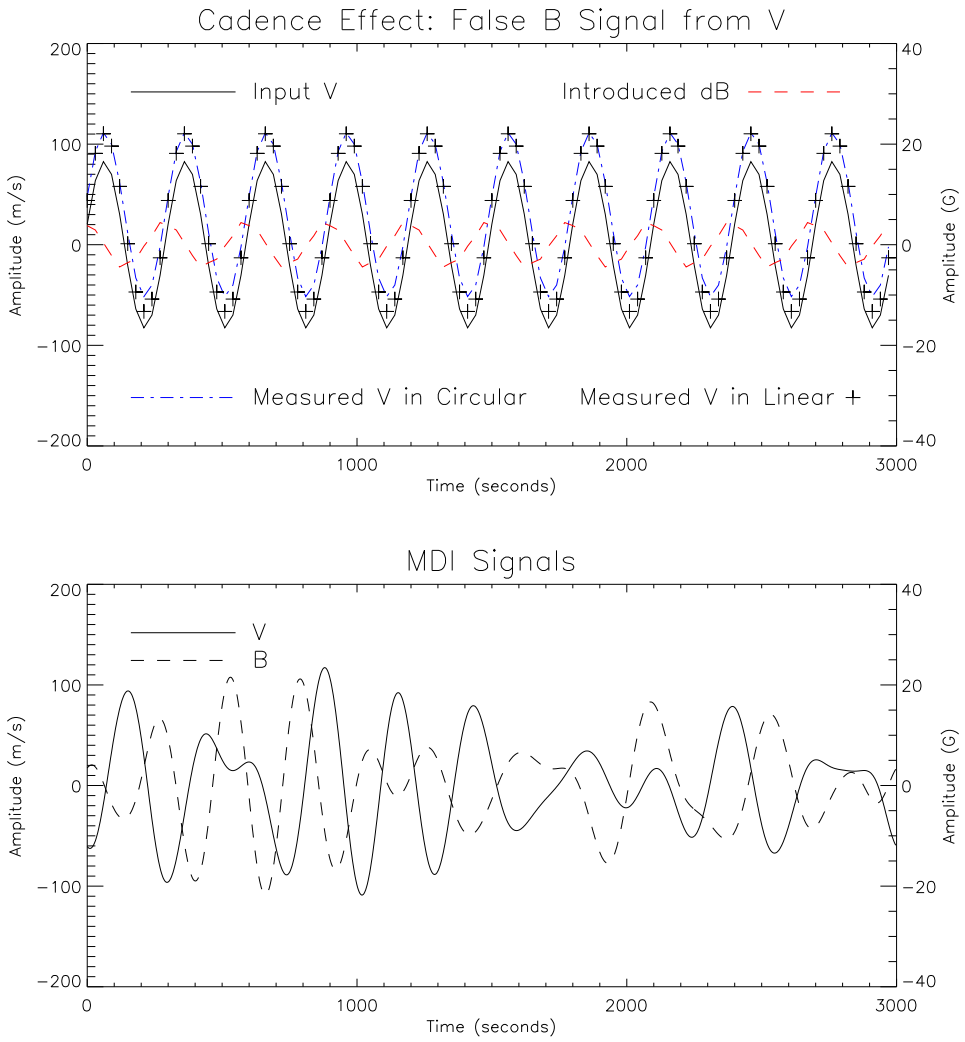

Fig. 18.— Upper panel provides an example of the 'Cadence Effect'. Solid line represents an artificial sinusoidal velocity with a 300 second period. The velocity is sampled every 3 seconds in accordance with MDI filtergram sampling rate. The 2000 Gauss field line profile is shifted in wavelength for each filtergram sampling. This simulates a distortion in the line profile over the MDI measurement time (30 seconds) caused by p-modes. The MDI algorithm is simulated producing a measure of B in time (minus average field strength) shown as dotted red line. Therefore, the cadence effect introduces an oscillation of the field. Lower panel plots the MDI signals as measured in a hi-res pixel of 1355 Gauss.

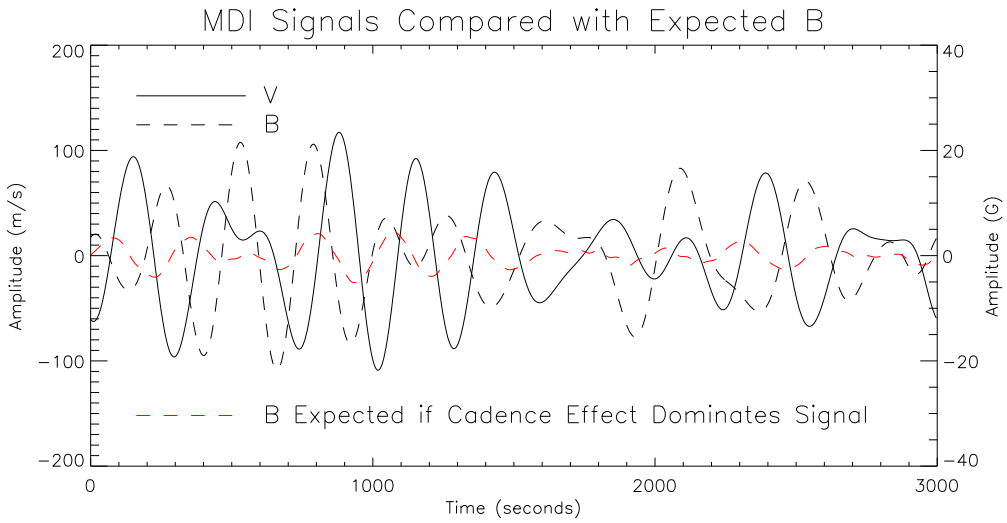

Fig. 19.— MDI signals (also shown in lower panel of previous figure) are plotted to compare with B signal expected from the 'Cadence Effect'. The velocity (solid line) is interpolated onto a 3 second time grid and used to shift the line profile an appropriate amount at each filtergram measurement. The produced B oscillation (red dotted line) from shifting a 1355 G line profile according to the velocity and sampling the filtergrams at the MDI cadence does not mimic the B signal as measured by MDI. I hand selected a pixel whose (v, dB) phase was exactly that expected from the cadence effect, therefore this example represents the worst case scenario, or the data most likely contaminated. (In reality, (v, dB) phases in MDI data have a wide range of values.) The expected B amplitude is often less than half of the observed amplitude, as well as being out of phase. It does not appear that the MDI B oscillation is heavily contaminated by this effect.

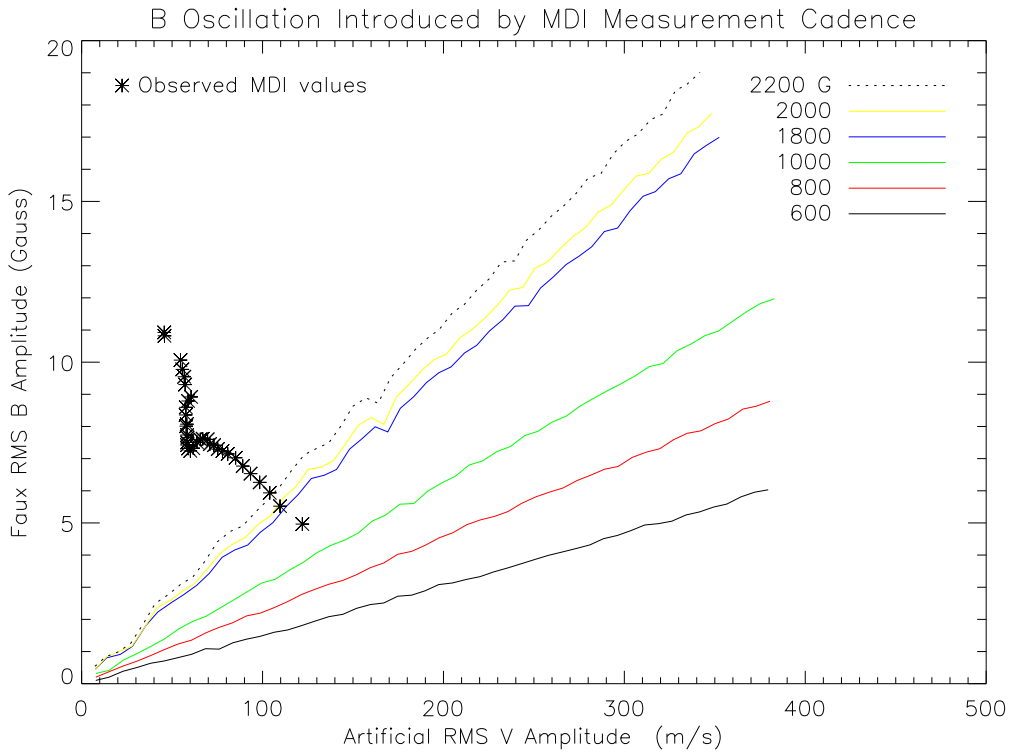

Fig. 20.— Faux RMS magnetic amplitudes are plotted as a function of RMS amplitudes of artifical velocity oscillations with a 300 second period. This work is done in order to simulate line profile distortions over time caused by p-modes. The introduced error (which appears as an oscillation of the magnetic field strength signal) is measured as an RMS amplitude and shown for line profiles of varying field strengths. Observed RMS signals from MDI data are plotted as points for comparison. The plotted symbols represent data from pixels whose average field values are 25 Gauss (lower right), 75, 125, 175...up to 1725 Gauss for the symbol at upper left. MDI magnetic data does not appear to be dominated by this cadence effect. Also, realistic velocity values for the data appear to be those values less than 200 m/s.

6. Sensitivity

The shutter noise is caused by uncertain exposure time that introduces error in measurement. SOHO/MDI has a shutter noise about 10-15 microseconds so that the intensities F1-4 wouldn't be measured exactly in the same duration. That noise will add a certain backgroud value to observables, and is therefore called 'offset' .

This offset in magnetograms has been corrected by using Gaussian fitting method. The sample data is collected from a magnetogram and the distribution of magnetic strength is computed. Assuming the small value data in this sample are purely noise and have a gaussian distribution, we use gaussian function to fit this distribution. The shift of the gaussian center would be the 'offset' introduced by shutter noise. Other fitting functions, such as two gaussian functions, three gaussian functions, are also used to fit the tails of the distribution that is believed to be contributed by true magnetic field (see Figure 21). The result is similar. Moreover, test is also done by selecting different parts of the magnetogram and different maximium values above which the data are abandoned. The offset almost keeps constant (see Figure 22), indicating this method is effective and reliable.

With correction of offset, the mean field of magnetic field was calculated and it is much smoother, showing the noise has been greatly minimized (see Figure 23). Possible residual magnetic signals in offset are corrected using wavelet technique. The noise level of MDI magnetic field is 16 Gauss for 1 minute magnetograms, and 9 Gauss for 5 minute magnetograms. The shutter noise introduces a 0.5 Gauss uncertainty.

The average and offset of 5 minute magnetograms are systematically 0.4 Gauss lower than those of 1 minute magnetograms (see Figure 24). It could be removed if the offset is corrected from observables. This difference may be caused by different observation sequences.

The correction of offset in Dopplergrams has not been done.

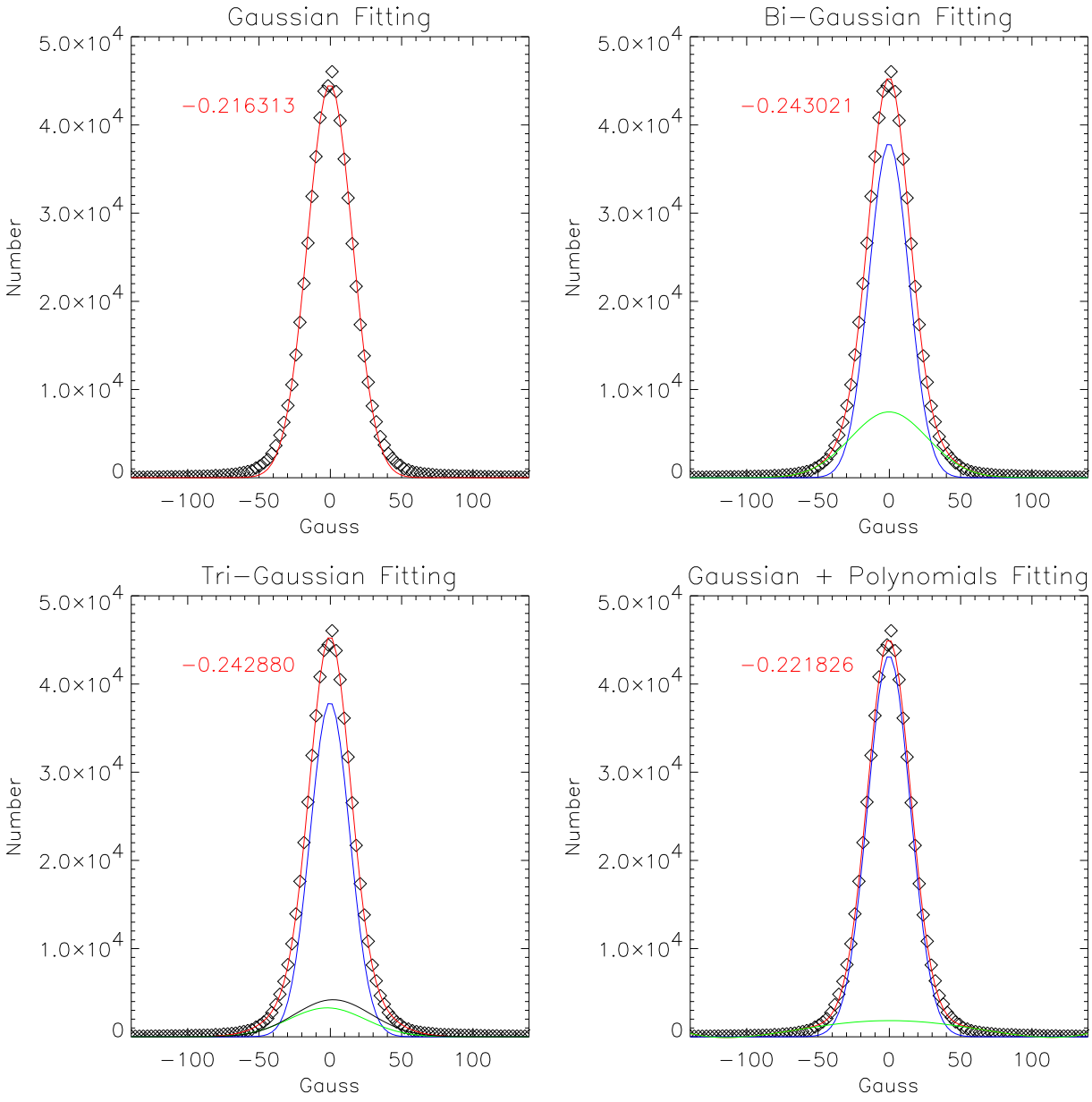

Fig. 21.— The fitting of observation using different fitting functions. The diamont is observed data and the red line is the final results to fit the observation. Other color lines represent the functions when more than one functions are used.

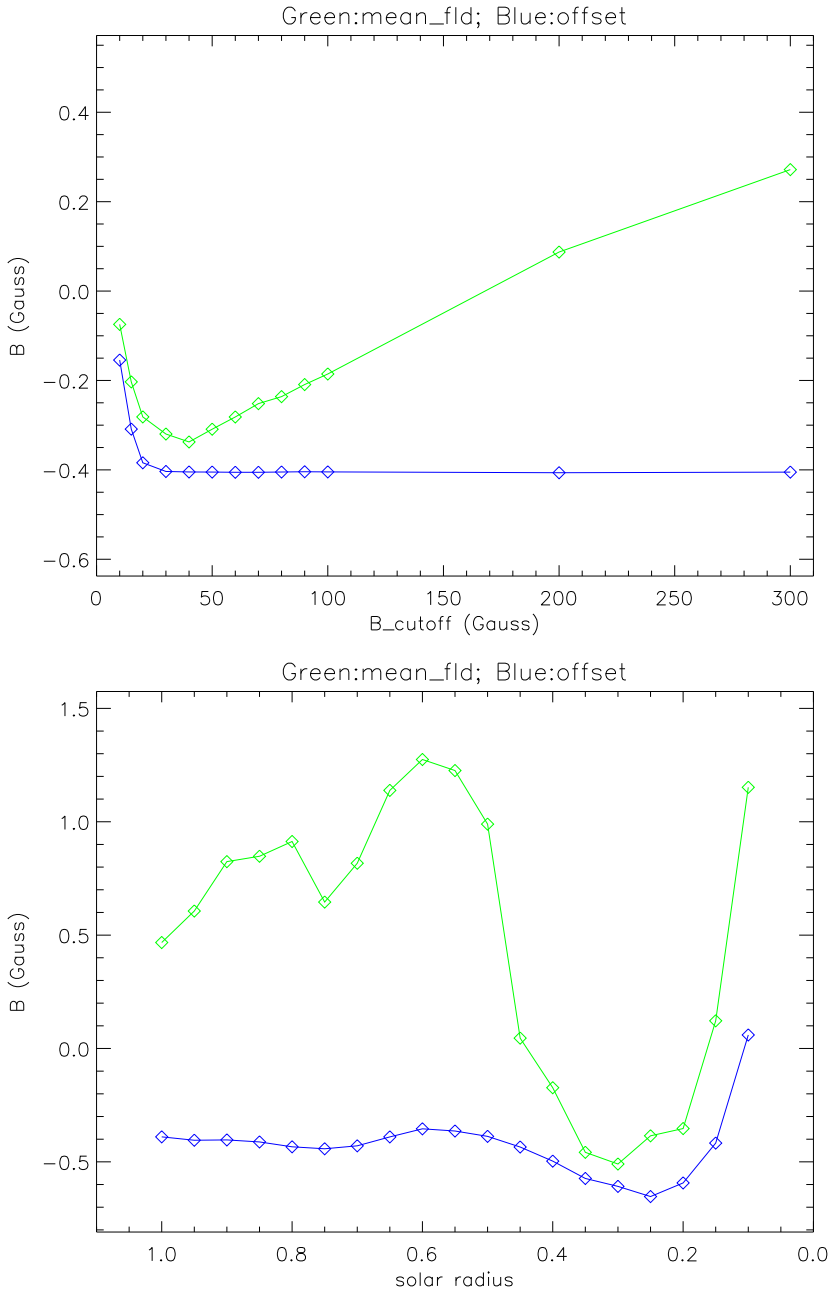

Fig. 22.— upper panel: magnetic mean field and offset versus the maxmium value above which the data are abondaned; lower panel: mean field and offset versus solar radius beyond which the data are abondaned.

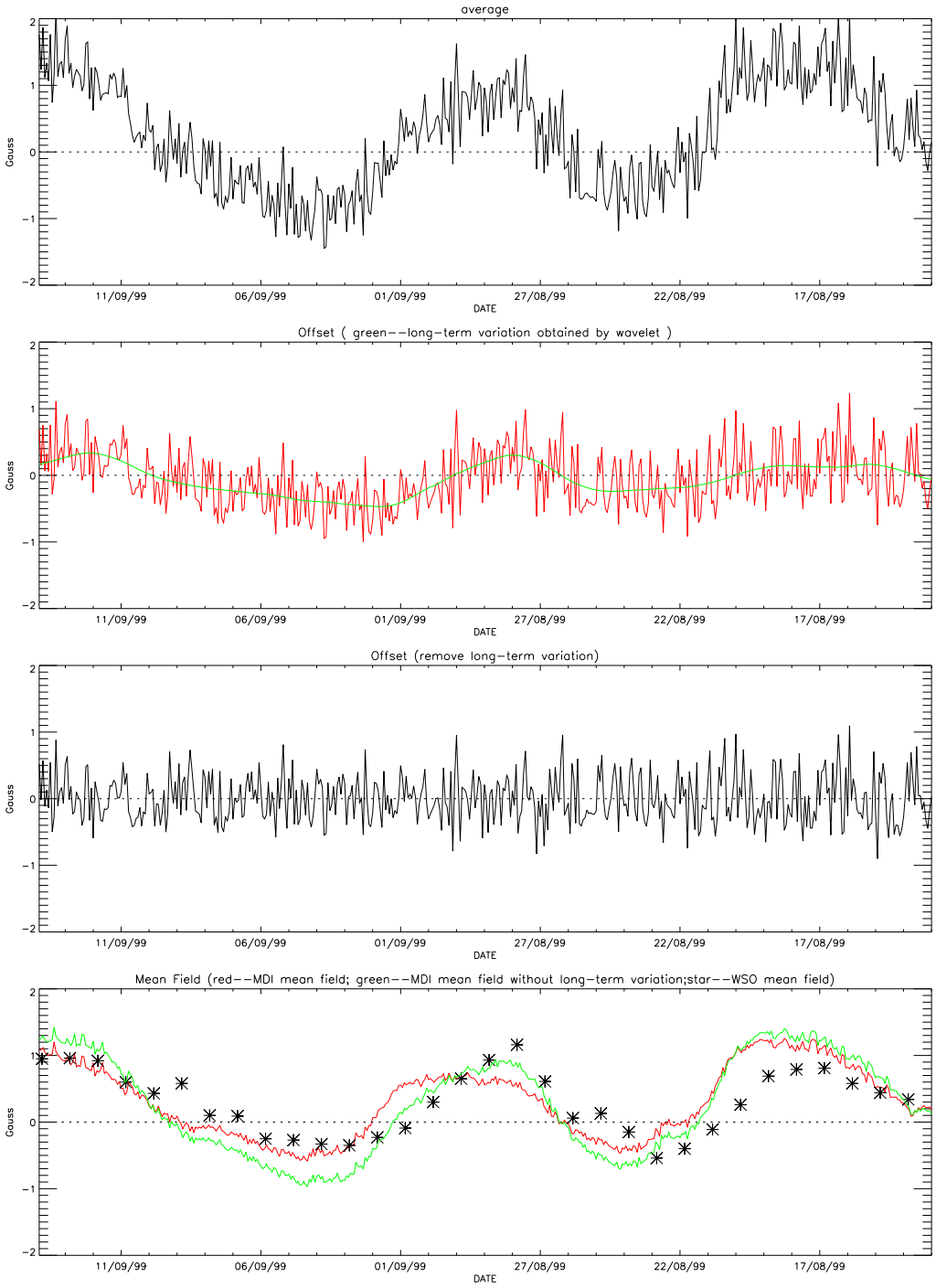

Fig. 23.— top panel: average; second panel: offset with long term variation; third panel: offset without long-term variation; bottom panel:mean field.

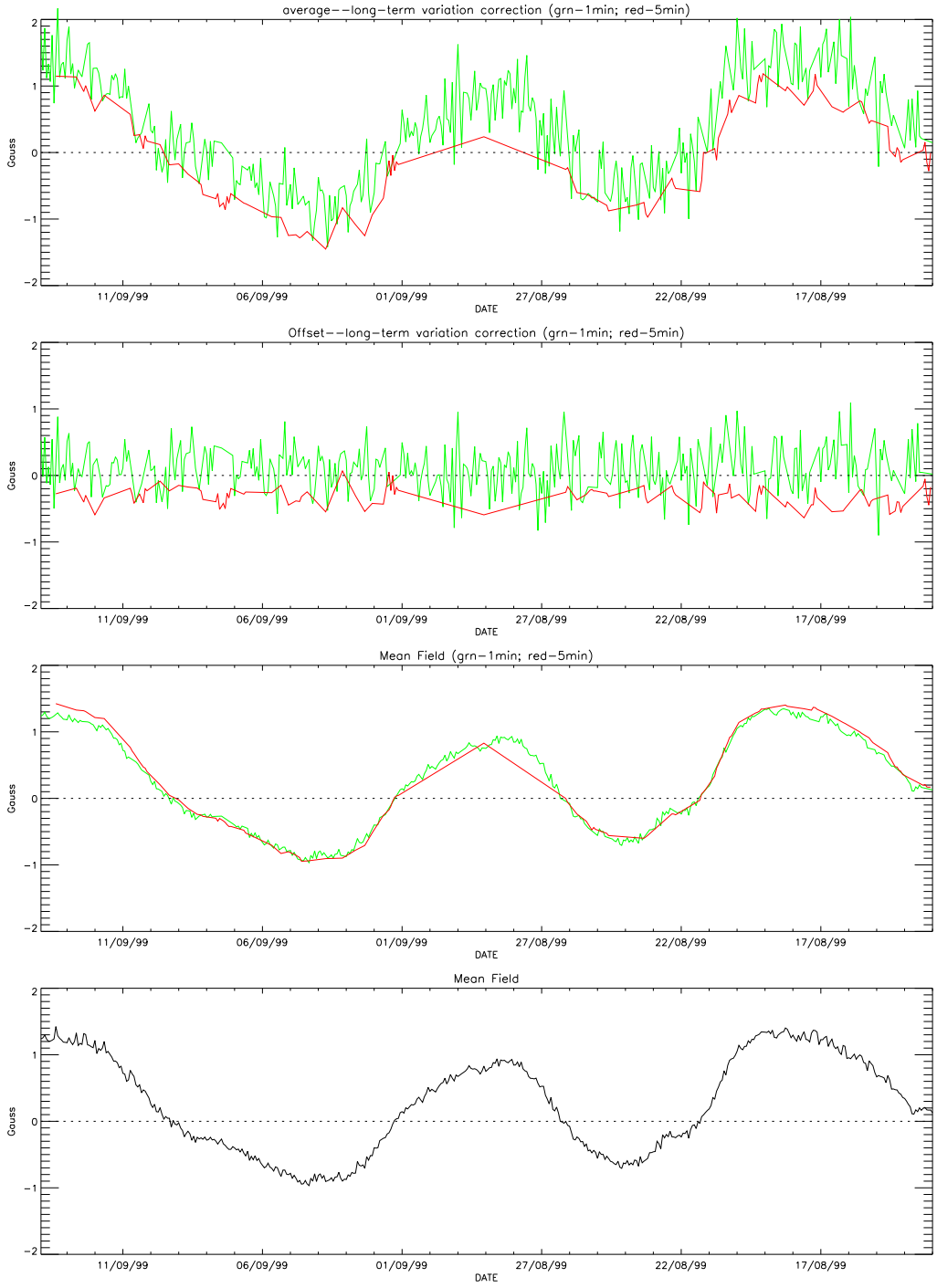

Fig. 24.— red–5min magnetograms; green–1min magnetograms. Bottom panel: mean field with both 5min and 1min data.

REFERENCES

Bellot Rubio, L.R., Collados, M., Ruiz Cobo, B., & Rodriguez Hidalgo, I. 2000, ApJ, 534, 989

Bruls, J.H.M.J., 1993, A & A, 269, 509

Giggerich, O., Noyes, R.W., Kalkofen, W., & Cuny, Y., 1971, Solar Physics, 18, 347

Lites, B., 1991, ApJ, 373, 683

Maltby, P. Avrett, E.H., Carlsson, M., Kjeldseth-Moe, O., Kurucz, P.L., & Loeser, R., 1986, ApJ, 306, 284

Martinez and Vazquez, 1991, A&A, 170, 494

Norton, A.A., 2000, Ph.D. Dissertation, "Study of Solar Photospheric MHD Oscillations", 45

Norton, A.A, Ulrich, R.K, and Liu, Y., 2001, ApJ, 561, 1

Pierce, A. K., & Slaughter, C. D., 1977, Solar Physics, 51, 25

Rabello-Soares, M.C., Korzennik, S.G., & Schou, J., 2001, Proc. SOHO 10/GONG 2000 Workshop, ESA-SP 464

Scherrer, P.H, Bogard, R., Bush, R., Hoeksema, J., Kosovichev, A., Schou, J., and Rosenberg, W., Springer, L, Tarbell, T., Title, A, Wolfson, C., Zayer, I, and the MDI Engineering Team, 1995, Solar Physics, 162, 129

Settele, A., Carroll, T., and Nickelt, I., 2001, A&A, submitted

This preprint was prepared with the AAS LaTeX macros v5.0.